

PREPARED FOR SUBMISSION TO JCAP

# LHC prospects for minimal decaying Dark Matter

**Giorgio Arcadi, Laura Covi and Federico Dradi**

Institute for Theoretical Physics, Georg-August University Göttingen, Friedrich-Hund-Platz 1,  
Göttingen, D-37077 Germany

**Abstract.** We study the possible signals at LHC of the minimal models of decaying dark matter. Those models are characterized by the fact that DM interacts with SM particles through renormalizable coupling with an additional heavier charged state. Such interaction allows to produce a substantial abundance of DM in the early Universe via the decay of the charged heavy state, either in- or out-of-equilibrium. Moreover additional couplings of the charged particle open up decay channels for the DM, which can nevertheless be sufficiently long-lived to be a good DM candidate and within reach of future Indirect Detection observations. We compare the cosmologically favored parameter regions to the LHC discovery reach and discuss the possibility of simultaneous detection of DM decay in Indirect Detection.

---

## Contents

<b>1</b>	<b>Introduction</b>	<b>1</b>
<b>2</b>	<b>The model</b>	<b>2</b>
<b>3</b>	<b>Collider analysis</b>	<b>4</b>
3.1	Colored scalar	6
3.2	EW-charged scalar	14
<b>4</b>	<b>Discussion</b>	<b>20</b>
<b>5</b>	<b>Conclusions</b>	<b>23</b>

---

## 1 Introduction

After the first run of the LHC, no signal of New Physics has been found yet in the traditionally DM-motivated channels containing missing energy [1, 2]. While the next LHC run could still bring a WIMP-like signal, especially from the electroweakly charged sector, we would like here to consider a different type of scenario, connected to the cosmologically well-motivated case of decaying Dark Matter.

In fact, it is perfectly possible that the DM particle is not stable, but just very long-lived and in such case immediately two usual DM assumptions are lifted: a) no symmetry is introduced to justify the stability of Dark Matter and therefore the particle can interact also as single state with charged SM and non-SM states; b) to ensure survival until the present age, the DM particle has to interact with suppressed couplings to any sector and therefore can be naturally produced not through the WIMP mechanism, which relies on electroweak-size cross-section, but via the FIMP or SuperWIMP mechanisms, based on much smaller couplings.

A very minimal setting of this type has been recently proposed in [3], featuring a DM Majorana fermion and a scalar charged under the SM gauge group. It is minimal in the sense that just a minimal particle content has been added to the SM and that the additional couplings are all renormalizable. Such a scheme can be embedded in more complex models, like supersymmetry with R-parity violation, but the main phenomenological characteristics are independent from the particle physics framework, at least for what concerns DM phenomenology. We will thus here concentrate on such minimal constructions as the more conservative case, since in the presence of a larger field content or more couplings, additional signals could be accessible at LHC or in DM indirect detection.

Due to the long lifetime of the DM, requiring at least one of the additional charged particles to be within the LHC reach constrains all couplings to be suppressed and therefore points also to regions of (near)-collider-metastability for these exotic states. It is therefore natural to look for such particles at the LHC in the presence of displaced vertices or metastable tracks (MP). These channels have recently attracted more attention [4–15] and are indispensable in order to cover a wide range of cosmologically interesting scenarios [16–23] like the one presented here.

This paper is organized as follows: we will discuss the type of minimal models we study in section 2 together with the connection to DM indirect detection and the DM production mechanisms. We will then study in section 3 the LHC phenomenology in the two scenarios of scalar field carrying color or only electroweak charge. Section 4 will be then devoted to the discussion of the results while our conclusions will be given in Section 5.

## 2 The model

We consider here the minimal model introduced in [3] (see also [24–26] for similar setups) featuring a Majorana fermion, singlet with respect to the SM gauge group and dark matter candidate, and a single scalar field multiplet  $\Sigma_f$ , non-trivially charged under at least one of the SM gauge groups. We assume that these fields interact among themselves and with the SM only via renormalizable Yukawa-type couplings according to the quantum number chosen for  $\Sigma_f$ . In particular the interaction between the DM and  $\Sigma_f$  will be of the form:

$$L_{\text{eff}} = \lambda_{\psi f} \bar{\psi} f \Sigma_f^\dagger + h.c. \quad (2.1)$$

where  $\psi$  is the DM Majorana fermion,  $f$  any chiral SM fermion and  $\Sigma_f$  denotes a scalar with quantum numbers equal to  $f$ .

No symmetry is imposed to guarantee the stability of the DM, allowing couplings of  $\Sigma_f$  with only SM fermions. Depending on the quantum numbers a rather broad variety of operators may arise:

$$\begin{aligned} L_{\text{eff}} &= \lambda_{1q} \bar{d} \ell \Sigma_q + h.c. & \Sigma_q &= (3, 2, 1/3) \\ L_{\text{eff}} &= \lambda_{1u} \bar{d} d^c \Sigma_u^\dagger + h.c. & \Sigma_u &= (3, 1, 4/3) \\ L_{\text{eff}} &= \lambda_{1d} \bar{q} \ell^c \Sigma_d + \lambda_{2d} \bar{u} d^c \Sigma_d^\dagger + \lambda_{3d} \bar{u} e^c \Sigma_d + \lambda_{4d} \bar{q} q^c \Sigma_d^\dagger + h.c. & \Sigma_d &= (3, 1, -2/3) \\ L_{\text{eff}} &= \lambda_{1\ell} \bar{e} \ell \Sigma_\ell + \lambda_{2\ell} \bar{d} q \Sigma_\ell + \lambda_{3\ell} \bar{u} q \tilde{\Sigma}_\ell + h.c. & \Sigma_\ell &= (1, 2, -1) \\ L_{\text{eff}} &= \lambda_{1e} \bar{\ell} \ell^c \Sigma_e + h.c. & \Sigma_e &= (1, 1, -2) \end{aligned} \quad (2.2)$$

where  $q, \ell$  denote the SM  $SU(2)_L$  LH doublets, while  $u, d, e$  are RH  $SU(2)_L$  singlets, and the superscript  $c$  indicates the charge-conjugated field,  $f^c = C \bar{f}^t$  while  $\tilde{\Sigma}_f \equiv i\sigma_2 \Sigma_f^*$ . On the right the quantum numbers of the  $\Sigma_f$  fields are specified according to the SM gauge groups  $SU(3)_c \times SU(2)_L \times U(1)_Y$ . We are here suppressing flavour indices, even if some couplings like  $\bar{q} q^c, \bar{\ell} \ell^c$  must be antisymmetric in flavour and vanish for a single generation, and considering in each line the presence of a single scalar field  $\Sigma_f$ . We have then that the new particle sector can just be described by two mass scales  $m_\psi$  and  $m_\Sigma$  and a few Yukawa couplings. The scalar field  $\Sigma_f$  is also coupled, according to its assignment of quantum numbers, given above, to the SM group gauge bosons.

The interactions (2.1) and (2.2) induce three-body decays for the Dark Matter with a rate given by, up to kinematical and multiplicity factors:

$$\Gamma_{\text{DM}} = \frac{c_f |\lambda_{\psi f}|^2 |\bar{\lambda}|^2}{384(2\pi)^3} \frac{m_\psi^5}{m_{\Sigma_f}^4}, \quad \bar{\lambda} = \lambda_{if}, \quad i = 1, \dots, 4, \quad f = q, u, d, \ell, e \quad (2.3)$$

with  $c_f$  = counting the number of degrees of freedom of the intermediate  $\Sigma_f$  ( $c_f = 6, 3, 3, 2, 1$  for  $\Sigma_q, \Sigma_u, \Sigma_d, \Sigma_\ell, \Sigma_e$  respectively). The decay channels can be different depending on the

quantum numbers of the intermediate particle  $\Sigma_f$ . We distinguish substantially four types of decay channels:

$$\begin{aligned}
\psi &\rightarrow \bar{u}u\nu, \bar{d}d\nu && \text{for } \Sigma_d, \Sigma_\ell \\
\psi &\rightarrow \bar{u}dl && \text{for } \Sigma_q, \Sigma_d \\
\psi &\rightarrow udd && \text{for } \Sigma_u, \Sigma_d \\
\psi &\rightarrow \bar{l}l\nu && \text{for } \Sigma_\ell, \Sigma_e
\end{aligned} \tag{2.4}$$

For simplicity we focus on signals of the type  $f\bar{f}\nu$  with  $f$  being either a quark or a charged lepton of any generation, denoted by  $l$ . We will also assume that the decays of DM are flavour conserving. If this is not the case bounds from flavour violation decays of mesons and leptons arise (see e.g. [27] for a complete list). However they are sensitively weaker than the one imposed by cosmology and DM ID. We will also assume that, for a given assignment of the quantum numbers of  $\Sigma_f$ , only one of the allowed operators, as reported in (2.2), dominates. We just comment that some of the effective lagrangians (2.2) violate both lepton and baryon number and in case of contemporary presence of lepton and baryon number violating operators, very strong constraints from the stability of the proton arise [28]. We will neglect here this possibility.

All the considered DM decay channels are already severely constrained from Indirect Detection. The hadronic decay channels, namely  $\bar{d}d\nu$  and  $u\bar{u}\nu$  are mostly constrained by antiproton searches, which give bounds on the DM lifetime varying between  $10^{26} - 10^{28}$  s for  $m_\psi > 100$  GeV [26] and can become as stringent as  $10^{29}$ s for values of the DM mass down to 1 GeV [29]. In the case of the leptonic decays, comparably severe constraints, ranging from approximately  $10^{27}$ s to  $10^{29}$ s, according to the decay channel, for DM masses between 10 GeV and 2 TeV, are obtained by the recent measurements by AMS of the positron flux and positron fraction [30]. In the case of the  $\Sigma_\ell$  mediator, one-loop induced decay processes in  $Z\gamma$  and  $\nu\gamma$  may also be important. In particular the latter can originate monochromatic  $\gamma$ -ray lines. Current searches give bounds which can be as strong as  $10^{29\div 30}$  seconds for  $m_\psi = 1 - 10$  GeV [24, 31, 32]. All these bounds can be satisfied only for a very small value of the product of the couplings, namely  $\lambda_{\psi f} \bar{\lambda} \lesssim 10^{-(16\div 22)}$ , for masses of the scalar field  $\Sigma_f$  within the kinematical reach of the LHC.

While the present lower limits on the DM lifetime only constrain the product of the couplings, the DM production mechanisms in the early universe also provide bounds on the ratio of the couplings. In fact, in this kind of models, the correct amount of DM relic density can be generated from the decays of the field  $\Sigma_f$  either in thermal equilibrium (freeze-in production [19, 33–36]) or out-of-equilibrium (SuperWIMP production [37–39])<sup>1</sup>.

Since the two processes take place at quite different cosmological epochs, the DM relic

---

<sup>1</sup>It is as well possible, alternatively, that the DM acquires its relic density through the WIMP paradigm. However this setup corresponds to the simple scenario with  $\lambda_{\psi f} \sim O(1)$  and an irrelevant coupling of  $\Sigma_f$  to SM fields. We will not consider this possibility in this work (see instead e.g. [40] for a scenario of this kind with DM coupling to the top quark).

density can be expressed, in very good approximation, as the sum of the two contributions [3]:

$$\begin{aligned}
\Omega_{\text{DM}} h^2 &= \Omega_{\text{DM}}^{\text{FI}} h^2 + \Omega_{\text{DM}}^{\text{SW}} h^2 \\
&\approx 1.09 \times 10^{27} \frac{g_\Sigma}{g_*^{3/2}} \frac{x \Gamma(\Sigma_f \rightarrow fDM)}{m_\Sigma} + x Br(\Sigma_f \rightarrow fDM) \Omega_\Sigma h^2 \\
&\approx x Br(\Sigma_f \rightarrow fDM) \left[ 0.717 \frac{g_\Sigma}{g_*^{3/2}} \left( \frac{1\text{s}}{\tau_\Sigma} \right) \left( \frac{1\text{TeV}}{m_\Sigma} \right) + \Omega_\Sigma h^2 \right]
\end{aligned} \tag{2.5}$$

where  $x = \frac{m_\psi}{m_\Sigma}$ ,  $g_\Sigma$  and  $g_*$  are, respectively, the internal degrees of freedom of the field  $\Sigma_f$  and the relativistic degrees of freedom of the primordial plasma at the time of DM production,  $\tau_\Sigma$  is the lifetime of the  $\Sigma_f$  field defined, up to kinematical factors, as:

$$\tau_\Sigma^{-1} = \Gamma_\Sigma = \frac{|\lambda_{\psi f}|^2 + |\bar{\lambda}|^2}{8\pi} m_\Sigma \tag{2.6}$$

while  $\Gamma(\Sigma_f \rightarrow fDM)$  and  $Br(\Sigma_f \rightarrow fDM)$  are the decay rate and branching fraction of the field  $\Sigma_f$  into DM. Neglecting the final state masses, we have then:

$$\Gamma(\Sigma_f \rightarrow fDM) = \frac{|\lambda_{\psi f}|^2}{8\pi} m_\Sigma, \quad Br(\Sigma_f \rightarrow fDM) = \frac{|\lambda_{\psi f}|^2}{|\lambda_{\psi f}|^2 + |\bar{\lambda}|^2} \tag{2.7}$$

We note that the freeze-in contribution is proportional to the decay rate of  $\Sigma_f$  into DM, which is in turn proportional to  $\lambda_{\Sigma f}$ , independently of the other coupling, while the SuperWIMP contribution depends on the branching fraction of decay of  $\Sigma_f$  into DM as well as on its mass and charge, strongly influencing the relic density  $\Omega_\Sigma h^2$ . But in general from eq. (2.5) we see that both production mechanisms are inefficient if the branching fraction of  $\Sigma_f$  decay into DM becomes too small. On the other hand a too large DM coupling to  $\Sigma_f$  can easily cause overproduction. Imposing the cosmological value of the Dark Matter density for  $\psi$  fixes some definite ranges of the couplings  $\lambda, \bar{\lambda}$  or equivalently  $\tau_\Sigma, Br(\Sigma_f \rightarrow fDM)$  as a function of the mass scales,  $m_\psi, m_\Sigma$ .

In the next sections we will investigate the reach of LHC in the detection of the charged field  $\Sigma_f$  and investigate which signal can be expected in the parameter regions favored by a successful cosmological DM production and possible DM decay.

### 3 Collider analysis

Contrary to the DM, the scalar field  $\Sigma_f$  is charged under SM gauge interactions which may give its efficient production at the LHC, if kinematically allowed. Since the Yukawa couplings with the quarks are much smaller than any of the gauge couplings, the main production channels at a proton-proton collider are gluon fusion into a scalar-antiscalar pair, for colored  $\Sigma_f$ , or Drell-Yan production, for the electroweakly or electromagnetically charged case. In either cases the production rate is practically independent on the details of the DM model, and given just by the mass and charge of the field  $\Sigma_f$ . We will estimate here the NLO production rates by computing the LO cross-section with the package MadGraph 5 [41] and correcting with a constant NLO k-factor, depending on the channel.

For any given assignment of its quantum numbers the scalar particle features two kind of decay channels after its production (We are implicitly assuming that in the case of the  $SU(2)$  doublets  $\Sigma_q$  and  $\Sigma_\ell$  the two components are mass degenerate. If this is not the case, in

addition to the processes described below, the decay of the heavier component of the doublet into a  $W$ , either on or off shell, and the lighter one is open. We will better clarify this point later in the text). We have first of all decays into a DM particle and a standard model fermion, with rate proportional to  $\lambda_{\psi f}^2$ , which can be classified as follows:

$$\begin{aligned}
\Sigma_f &\rightarrow u\psi & \text{for } \Sigma_q, \Sigma_u, \Sigma_d \\
\Sigma_f &\rightarrow d\psi & \text{for } \Sigma_q, \Sigma_d \\
\Sigma_f &\rightarrow l\psi & \text{for } \Sigma_\ell, \Sigma_e \\
\Sigma_f &\rightarrow \nu\psi & \text{for } \Sigma_\ell
\end{aligned} \tag{3.1}$$

where  $l$  is a charged lepton. We see that only in the case of  $\Sigma_\ell$  the decay can be into an invisible final state  $\nu\psi$ , but in that case also the visible channel into a charged lepton is present. So the decays in general give rise to a kink in the observable charged track/jet due to the  $\Sigma_f$  decay.

The scalar field can decay as well into two SM fermions, with a rate governed by  $\bar{\lambda}^2$ , according the following channels:

$$\begin{aligned}
\Sigma_f &\rightarrow q\bar{q}' & \text{for } \Sigma_u, \Sigma_d, \Sigma_\ell \\
\Sigma_f &\rightarrow ql & \text{for } \Sigma_q, \Sigma_d \\
\Sigma_f &\rightarrow q\nu & \text{for } \Sigma_q, \Sigma_d \\
\Sigma_f &\rightarrow \bar{l}l & \text{for } \Sigma_\ell \\
\Sigma_f &\rightarrow l\nu & \text{for } \Sigma_\ell, \Sigma_e
\end{aligned} \tag{3.2}$$

where  $l$  is, again, a charged lepton while  $q$  is an up or down-type quark. In view of the dependence of the decay rate of  $\Sigma_f$  on the  $\lambda_{\psi f}, \bar{\lambda}$ -type coupling, a tight relation exists between possible signals at LHC of such decays and the constraints from the DM phenomenology, being governed by the same couplings. As already argued in [3] the constraints from ID and from the cosmological abundance of the DM require very low values of the couplings, namely  $\lambda, \bar{\lambda} \lesssim 10^{-(7\div 8)}$ , thus implying that the decay vertices result displaced with respect to the production ones and may even lie outside the detector.

In order to determine the LHC capability of detecting this kind of decays we will adopt the method introduced in [42]. We have then identified three possible detection regions, referring for definiteness to the design of the CMS detector (see [43] for a detailed description of the detector), namely the Pixel and the Tracker (inner detector), and an “outside” region. The inner detector regions are sensitive to the shorter lifetimes and allow for the detection of displaced vertices (see for example [44], as well as [45] for similar searches from the ATLAS collaboration). The “outside” region is instead suitable for the detection of very long-lived particles, whose corresponding signal is constituted by outgoing tracks, thus related to the scalar field itself rather than its decays. On recent times searches of decay of stopped particles [46] in the detector have been considered as well. This is an very intriguing possibility since this last kind of searches result complementary to the ones of outgoing tracks. We will further comment on this later in the text.

We have generated several samples of pair produced  $\Sigma_f$ , at 14 TeV of centre of mass energy, corresponding to different assignments of its quantum numbers and different masses, and determined the spatial distribution of the decay vertices from the kinematic variables of the events and the decay rate  $\Gamma_\Sigma$  as described in [42]. Note that we consider here a straight-line motion of the particle after production, neglecting the magnetic field deflection

and the interactions with the intervening matter, which could even increase the number of decays in the inner part of the detector by bending the trajectory or slowing down the decaying particle <sup>2</sup>. Assuming 100 % detector efficiency, in order to claim the discovery for a given scenario we have required the presence of at least 10 decay events in one of the components in which the detector is schematized, i.e. in the pixel or the tracker, or outside the detector <sup>3</sup>. The optimal scenario, and thus main focus of our analysis, is however a “double” LHC detection scenario, consisting in the contemporary detection of at least 10 events in one of the components of the inner detector, namely pixel or tracker, and 10 tracks leaving the detector. This indeed would allow for a cross-check in the measurement of the lifetime of the scalar particle as well as a better discrimination of possible backgrounds.

For each of the cases considered we have performed the analysis for three definite luminosities, namely  $25 \text{ fb}^{-1}$ ,  $300 \text{ fb}^{-1}$  and  $3000 \text{ fb}^{-1}$ , in order to determine the feasibility of a next future discovery during run II, as well as the maximal discovery reach considering the full LHC data set and, finally, after a high luminosity run.

Since the analysis employed is not sensitive to the particular type of decay products of  $\Sigma_f$ , as long as a vertex (or kink) can be observed and happens in the detector, we will from now on refer to a schematic setup described by just four model parameters: the mass  $m_{\Sigma_f}$  of the scalar field, the ratio  $x = m_\psi/m_{\Sigma_f}$  and two couplings  $\lambda$  and  $\lambda'$ , referring, respectively, to the decay of  $\Sigma_f$  to the DM or to only SM states. We have as well considered an equivalent representation in terms of the  $\Sigma_f$  lifetime and DM branching fraction, more directly connected to the phenomenological observables at the LHC, and also helpful to translate the results obtained in different particle physics setups. In either case we will find the region of parameter space where displaced vertices and/or metastable tracks may be seen and compare it to the cosmologically viable parameter space.

As will be discussed later, it would be very important, in order to relate an hypothetical LHC signal to the DM properties, to distinguish both the decay channels of  $\Sigma_f$ . A necessary condition for the identification of a particular channel is that the product of the total number of events times the corresponding branching fraction is large enough, in one of the detector regions where it is possible to observe the decay products of the scalar field. A proper determination of the number of events needed would require the full detector simulation, accounting for the capability of reconstruction of the various decay products.

In the following subsections we will investigate separately the scenarios of color and electroweakly charged scalar particle.

### 3.1 Colored scalar

The first case that we are going to consider is when the field  $\Sigma_f$  carries color charge. Colored states are expected to be more efficiently produced at the LHC. For definiteness we will consider a  $\Sigma_d$ -type field in our analysis. As already mentioned, the  $\Sigma_{f=q,u,d}$  pairs are produced through gluon fusion and thus the production cross section is substantially the same for the three kind of states, apart a possible enhancement in the case of  $\Sigma_q$  because of multiplicity. We will indeed assume, for this scenario, that the two components of the doublet  $\Sigma_q$  are exactly degenerate in mass. If this is not the case the heaviest state of the doublet could decay into the lightest one and a W boson, if kinematically possible, or two quarks or leptons (through

---

<sup>2</sup>Such effects could be captured only by a full detector simulation, which is beyond the scope of this paper.

<sup>3</sup>Notice that this is a rather conservative requirement which prevents the effect of statistical fluctuations and ensures stable numerical results. For a pure Poisson distribution and no background 5 such events correspond to a discovery at the 95% CL.

an off-shell  $W$ ). For mass splittings above  $\sim 1$  GeV this decay channel has a branching fraction substantially equal to one and leads to prompt decays of the heavy state in case its production is accessible at the LHC. For sizable enough mass splittings, such that the momentum of decay products can survive analysis cuts (e.g. quality of signal requirements, background discrimination cuts), this decay can be detected and, then, the signals discussed in the following would result accompanied by prompt jets or leptons. On the other hand the required mass splitting would imply a sensitive suppression of the pair production of the heaviest states of the doublet and thus a small number of this kind of events. This might not be the case of the  $\Sigma_\ell$ -type particles, as will be clarified in the next subsection.

According to the method described above we have generated samples of events of  $\Sigma_d$  pair production normalizing the cross-section computed by Madgraph with a k-factor, accounting for NLO effects, which has been taken from the numerical package Prospino [47], given the similarities with the supersymmetric case of a stop squark. From the determination of the production cross-section it is possible to infer a general upper limit on the LHC reach at a given luminosity  $\mathcal{L}$ , from the relation  $N_{\text{ev}} = \sigma_{pp \rightarrow \Sigma_d \Sigma_d^*} \mathcal{L} \geq 5$  (10 events correspond to 5 pair produced  $\Sigma$ ) where  $N_{\text{ev}}$  represents the number of produced pairs  $\Sigma_d \Sigma_d^*$  irrespectively of the position of the decay vertices. For the luminosities considered in our analysis the LHC reach ranges from around 1600 GeV at  $\mathcal{L} = 25 \text{ fb}^{-1}$  to a maximal value of 2200 GeV corresponding to  $\mathcal{L} = 3000 \text{ fb}^{-1}$ . We have then computed the spatial distribution of the decay vertices for several values of the mass of  $\Sigma_d$ , namely 800, 1600 and 2200 GeV. Masses below 800 GeV are currently excluded, for the range of lifetimes relevant for our analysis, by current searches of detector stable particles [48, 49].

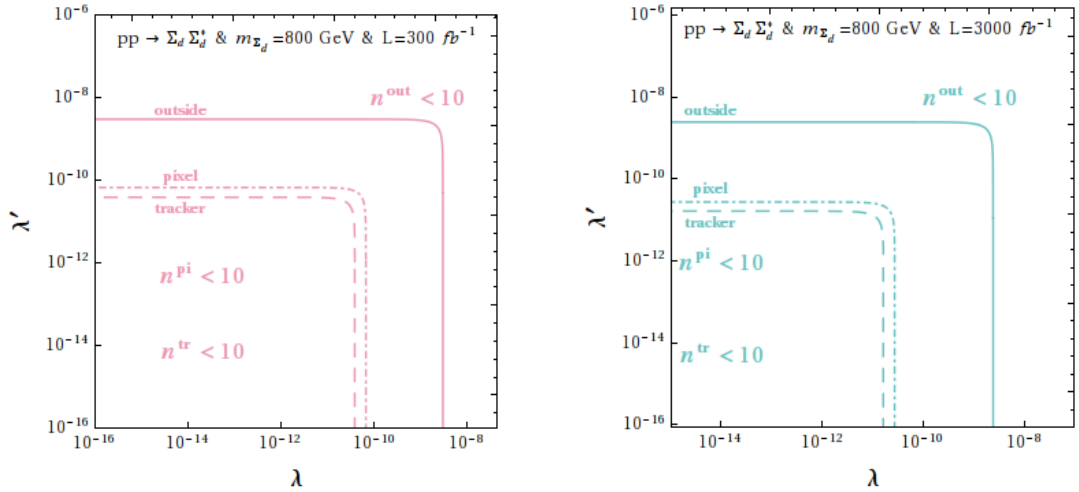


**Figure 1:** LHC reach in the plane of the pure SM  $\lambda'$  vs DM coupling  $\lambda$  for (from left to right)  $\mathcal{L} = 300, 3000 \text{ fb}^{-1}$  for  $m_{\Sigma_d} = 800$  GeV. The region below the solid line corresponds to at least 10 metastable tracks, while the regions above the dashed/dash-dotted lines to at least 10 decay events in the tracker or pixel detector respectively.

We report two examples of results of our analysis in fig. (1), for  $m_{\Sigma_d} = 800$  GeV and  $\mathcal{L} = 300, 3000 \text{ fb}^{-1}$ , where we have identified the region corresponding to more than 10 decay events in the pixel, tracker and outside the detector. We see that the contours run piecewise



parallel to the axis, since in most of the parameter space one single coupling dominates the total decay rate. The detection regions for pixel and tracker are very similar, since the difference in volume is practically compensated by the distance from the interaction point.

The searches for displaced vertices and particles escaping from the detector are highly complementary: the first has a maximal reach at low lifetimes, corresponding to high values of  $\lambda, \lambda'$ , while the latter is able to probe efficiently the very long lifetimes, i.e. low values of  $\lambda, \lambda'$ . Combining both search strategies allows to cover practically the whole parameter space.

The strong requirement of detection of both types of signal, i.e. displaced vertices in the pixel/tracker and metastable tracks, is realized only in the narrow regions comprised between the iso-contours in the plane  $(\lambda, \lambda')$  representing the detection of exactly 10 events in the pixel, tracker and outside the detector. The size of these strips is expected to increase with the integrated luminosity and, instead, to shrink once increasing the mass of the scalar, because of the lower number of particles produced. For the highest values of the mass, corresponding to approximately 2200 GeV the whole parameter space in the couplings might only be probed by the high luminosity upgrade of the LHC as long as both types of signal, either displaced vertex or metastable track, are considered.

The capability of LHC detection of a displaced decay of  $\Sigma_d$  or its metastable track can be confronted with the requirement of the correct cosmological DM abundance via  $\Sigma_d$  decay and, possibly, a detection of decaying DM. In case of a colored scalar the correlation between the DM phenomenology and the LHC predictions is rather straightforward since the DM production is substantially dominated by the first (freeze-in) contribution in eq. (2.5) and the couplings can be analytically determined as function of  $x$ ,  $m_{\Sigma_d}$  and the DM relic density and lifetime as [3]:

$$\begin{aligned}\lambda &\simeq 1.59 \times 10^{-12} x^{-1/2} \left(\frac{g_*}{100}\right)^{3/4} \left(\frac{\Omega_{\text{CDM}} h^2}{0.11}\right)^{1/2} g_{\Sigma}^{-1/2} \\ \lambda' &\simeq 0.91 \times 10^{-12} x^{-2} \left(\frac{g_*}{100}\right)^{-3/4} \left(\frac{m_{\Sigma_f}}{1 \text{ TeV}}\right)^{-1/2} g_{\Sigma}^{1/2} \left(\frac{\tau_{\psi}}{10^{27} \text{ s}}\right)^{-1/2} \left(\frac{\Omega_{\text{CDM}} h^2}{0.11}\right)^{-1/2}\end{aligned}\quad (3.3)$$

From these relations we can determine the cosmologically preferred parameter space in the plane of the couplings. We show indeed in fig. (2), as solid lines, the isolines of the correct value of the DM relic density for  $m_{\Sigma_d} = 800$  GeV and some values of  $x$  ranging from  $10^{-3}$  to 0.5. They appear as vertical lines since the freeze-in mechanism is independent from  $\lambda'$ . These curves can be confronted with the contours of the reach in the three detector regions. The panels of fig. (2) report the LHC reach for the three values of luminosity considered in our analysis. Fig. (3) shows an analogous analysis for the values  $m_{\Sigma_d} = 1600, 2200$  GeV. In this case we have considered only  $\mathcal{L} = 3000 \text{ fb}^{-1}$  since we expect a statistically relevant number of events only for this very high luminosity. In fig. (2) and (3) we have reported as well (dashed lines) the values of the DM lifetime, for the chosen combinations of parameters, near the present bounds. As already stated, we have assumed, for the scenario of colored scalar field,  $u\bar{u}(d\bar{d})\nu$  as the only relevant decay channel for the DM and thus applied the bounds of [26] in the  $m_{\psi} > 100$  GeV region and of [29]<sup>4</sup> at lower masses. For any value of  $x$ , the intersection of the corresponding solid and dashed lines corresponds to a DM with the

<sup>4</sup>The bounds presented here actually refer to two body decays in fermion pairs and then result conservative since in our setup part of the energy of the products is carried away by the neutrinos.

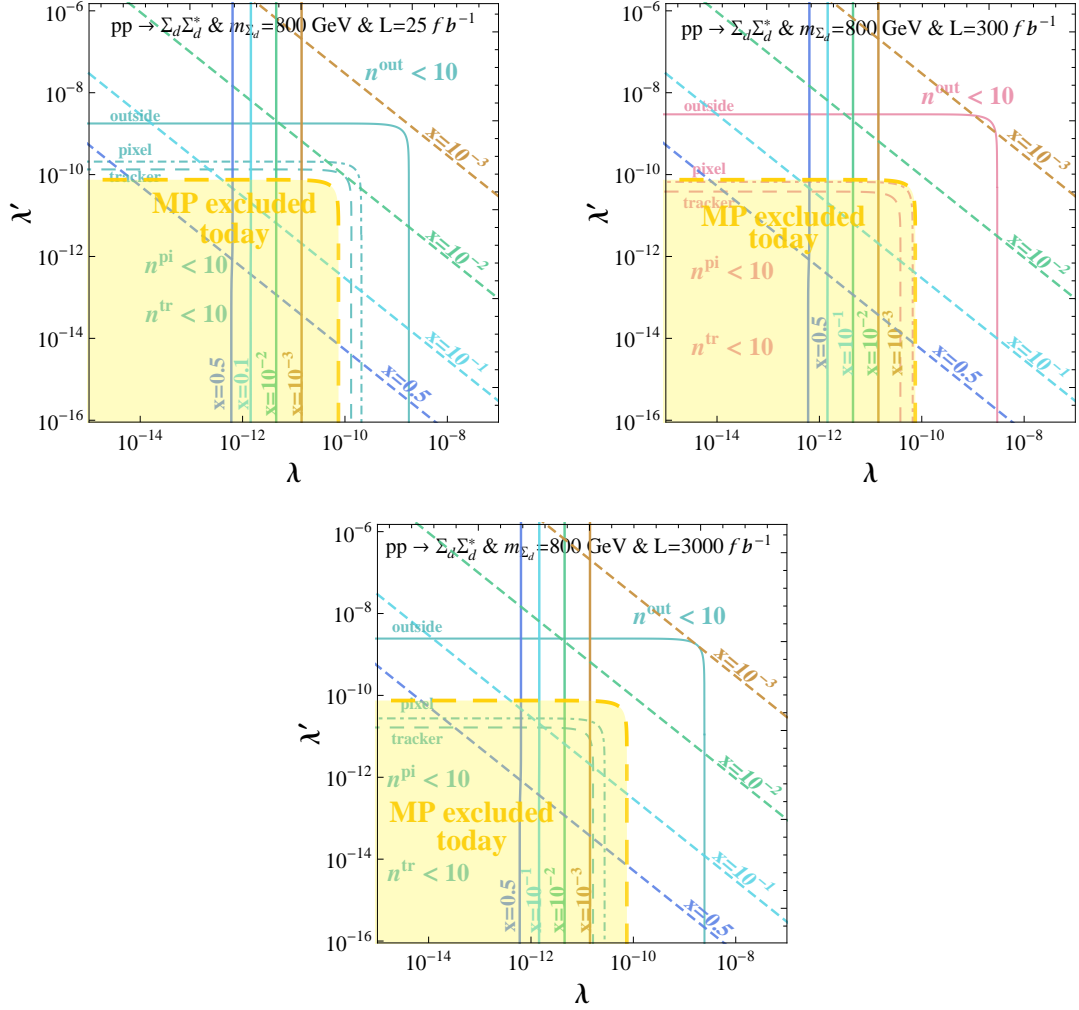


**Figure 2:** Contours of the correct DM relic density (solid lines) and of the reference value of  $10^{28}$ s of its lifetime (dashed lines) color-coded according to the values of  $x$  reported in the plot. A combined detection of  $\Sigma_d$  at LHC and of the DM candidate via ID can be achieved if the lines of the DM relic density and lifetime, corresponding to a given value of  $x$ , intersect within the discovery region between the iso-contours labeled as pixel-tracked and outside. The plot refers to  $m_{\Sigma_d} = 800$  GeV and  $\mathcal{L} = 25 \text{ fb}^{-1}$  (left plot),  $\mathcal{L} = 300 \text{ fb}^{-1}$  (left plot),  $\mathcal{L} = 3000 \text{ fb}^{-1}$  (bottom plot). The yellow shaded region delimited by the yellow thick long-dashed line is already excluded by current searches for metastable particles.

correct relic density and a lifetime approximately coinciding with the current observational bounds for the assumed dominant decay channel; consequently the parameter space above the DM lifetime curves may be already excluded. Notice that the actual ID exclusion region depends strongly on the DM decay channel and DM mass and is affected from astrophysical uncertainties in the propagation modeling as discussed in [26].

The most favorable scenario, consisting in a multiple detection of the DM and  $\Sigma_d$  decay, respectively in cosmic rays and at the LHC, with the latter satisfying the double LHC

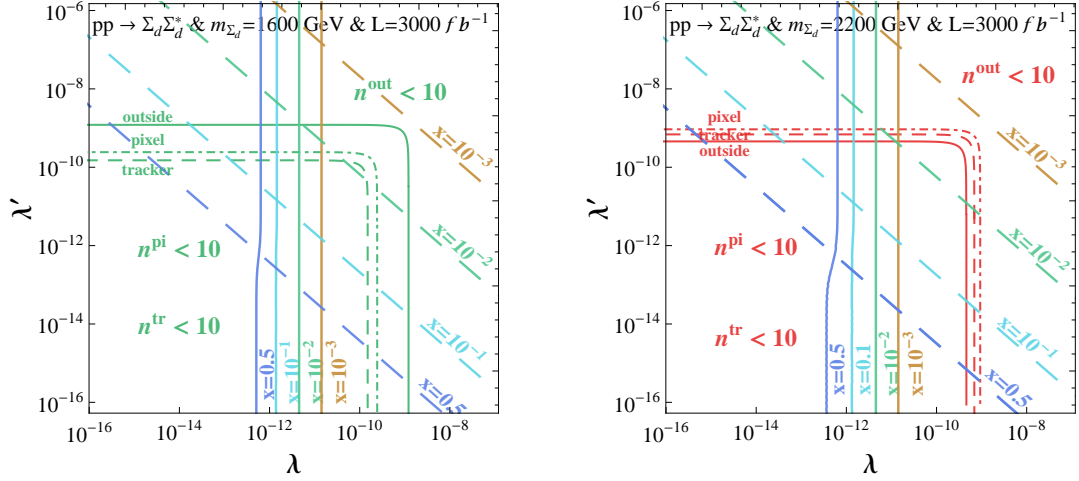


**Figure 3:** The same as fig. (2) but with  $m_{\Sigma_d} = 1600$  GeV (left plot) and  $m_{\Sigma_d} = 2200$  GeV (right plot) and  $\mathcal{L} = 3000\text{fb}^{-1}$  in both cases.

detection requirement, is potentially feasible, for a given value of the pair  $(x, m_{\Sigma_d})$ , when the corresponding isolines of the DM relic density and lifetime intersect inside the double detection region. Outside this region the contemporary ID detection of DM and only one type of LHC signal, i.e. displaced vertices (above the white strip) or metastable tracks (below the white strip), is anyway still feasible. We remark, however, that the region below the white strip, corresponding to very long lifetimes, is already constrained, for the lower values of the mass of the scalar, by current searches of detector stable particles. We have reformulated, for the scenario under consideration, these constraints using the procedure described in [42] and reported the excluded region in fig. (2). The region below the “double” detection strip is nearly ruled out for  $m_{\Sigma_d} = 800$  GeV. The limit from detector stable particles weakens very quickly with increasing mass of the scalar particle and it is substantially irrelevant for masses above 1 TeV.

The double LHC detection region corresponds, for  $m_{\Sigma_d} = 800$  GeV, to a rather definite range of values of  $x$  comprised between  $10^{-2}$  and  $10^{-1}$ . This range is reduced at higher values of  $m_{\Sigma_d}$  because of the decreased size of the LHC double detection strip. For the highest possible value  $m_{\Sigma_d}$  the combined detection prospects are substantially limited to  $x \simeq 10^{-2}$ .

It is also interesting to reformulate the previous results in a more model independent way in terms of the pair  $(\Gamma_{\Sigma}^{-1}(s), Br(\Sigma_d \rightarrow \text{DM}))$  as done in fig. (4), (5). Using these parameters the LHC detection regions are just delimited by horizontal lines of constant  $\Gamma_{\Sigma}$  values. The green (violet) shaded regions in the plot represent the regions in which it is possible to detect more than 10 events in the pixel/tracker (outside region). “Double” signals are accessible instead in the middle white strip. The combined LHC detection of the  $\Sigma_d$ , in at least one of the two channels, and DM indirect detection are again achieved whenever the isolines (dash-dotted) of the reference DM lifetime and of the correct relic density (solid) for a fixed value of  $x$  cross in the LHC “double” discovery region. Above this strip it is still possible to observe displaced vertices at the LHC and have an ID DM signal for small values of  $x$ . At large values of  $x$ , instead, only metastable particle signals are compatible with DM ID.

As evident from the plots, simultaneous ID/LHC detection, with the latter in the form

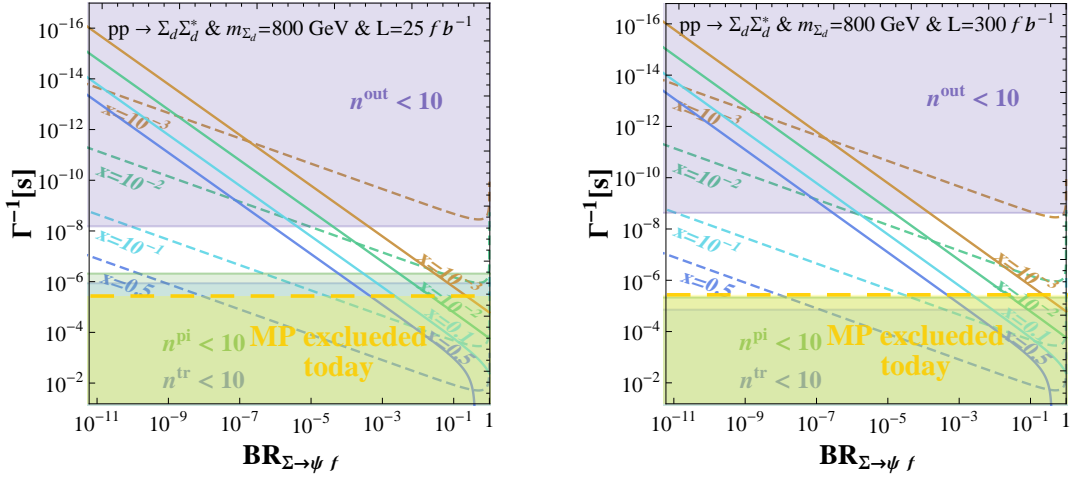


**Figure 4:** LHC detection reach compared with the constraints from DM phenomenology in the plane  $(Br(\Sigma_d \rightarrow \text{DM}), \Gamma_{\Sigma_d}^{-1})$ . The shaded green (magenta) region corresponds to more than 10 decay events happening in the pixel or tracker (outside the detector). The double detection region is the white strip comprised between the shaded regions. We have fixed  $m_{\Sigma_d} = 800 \text{ GeV}$  and  $\mathcal{L} = 25 \text{ fb}^{-1}$  (left plot) and  $\mathcal{L} = 300 \text{ fb}^{-1}$  (right plot). The yellow shaded region, below the thick long-dashed yellow line, is excluded by current bounds on metastable particles.

of a double signal, i.e. displaced decay plus metastable track, could be achieved in the next future, namely for luminosities up to  $300 \text{ fb}^{-1}$ , for values of  $Br_{\Sigma_d \rightarrow d\psi}$  lower than  $10^{-3}$ . As a consequence the observation at the LHC of both the DM and only SM decay channels of  $\Sigma_d$  appears difficult but it is not a priori excluded provided that there is a high statistics.

In order to investigate this possibility we have performed a more focused study on a benchmark set of parameters, namely  $m_{\Sigma_d} = 800 \text{ GeV}$ , corresponding to the maximal production cross-section,  $m_\psi = 10 \text{ GeV}$  and  $\lambda$  and  $\lambda'$  fixed to reproduce the correct DM relic density and a DM lifetime of approximately  $10^{28}$  seconds. We have reported on table (1) the number of decay events, expected at the three values of the luminosity, namely 25, 300 and  $3000 \text{ fb}^{-1}$ , together with an estimate of the number of events in the two different type of decay channels, namely in DM plus SM fermion and two SM fermions.

As evident, no events of decay into DM can be observed inside the detector (namely pixel or tracker), even in a high luminosity run of LHC. This is a consequence of the very suppressed branching ratio of decay of  $\Sigma_d$  into DM,  $\approx 10^{-3}$ , required to reconcile the correct DM relic density with observable decays of the latter. A potential observation of decay of  $\Sigma_d$  inside the detector seems thus limited to the pure SM channel. Possible dedicated searches should be then optimized for the search of displaced vertices with multi-jet/leptons and low amounts of missing energy.

The observation of the DM channel might be feasible considering the possibility of observing decays of stopped particles in the detector. Indeed we have until now assumed that the decays of  $\Sigma_d$  can be observed in the pixel/tracker region while beyond those only escaping tracks associated to the particle  $\Sigma_d$  itself are detected. In reality colored/electromagnetically charged metastable particles lose energy by interacting with the detector material and a frac-

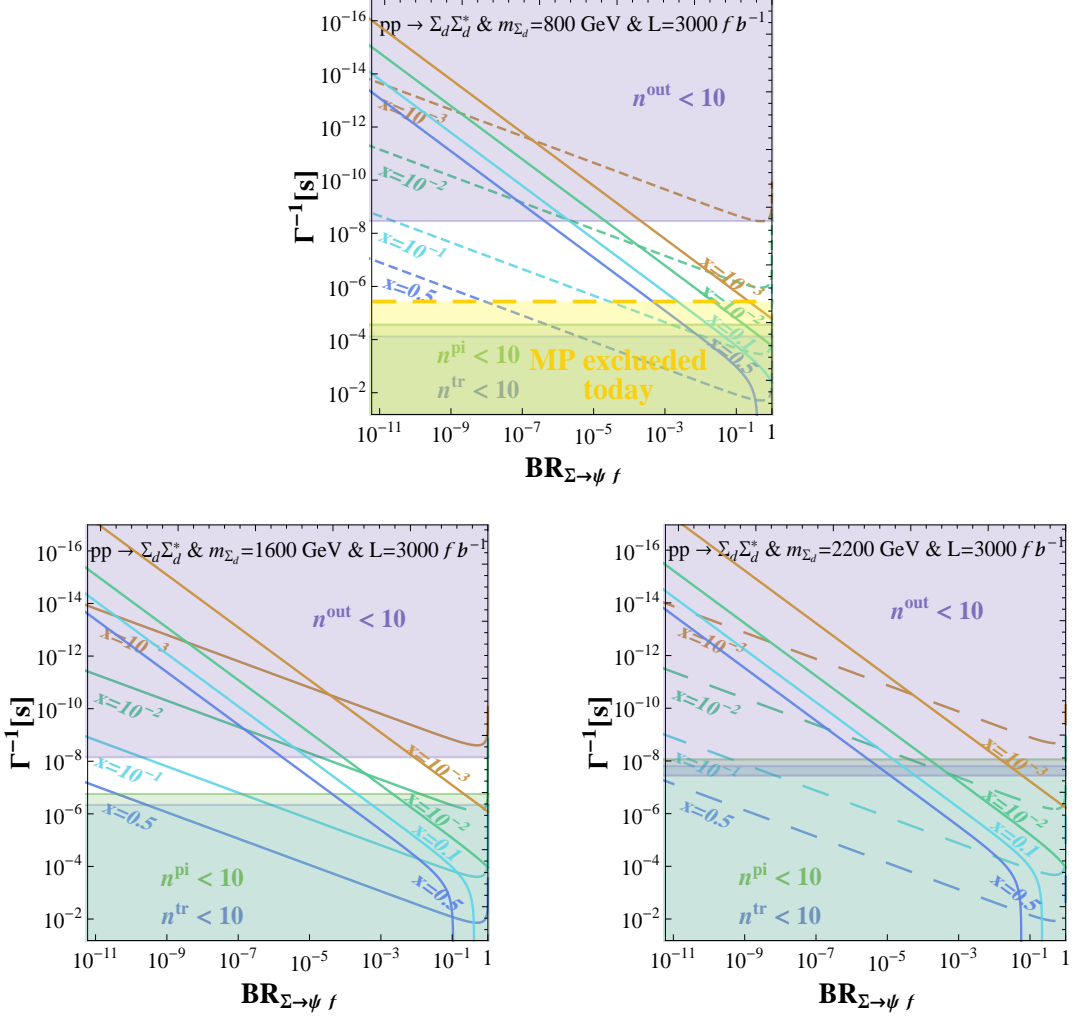


**Figure 5:** The same as fig. (4) but with  $m_{\Sigma_d} = 800$  GeV (upper plot),  $m_{\Sigma_d} = 1600$  GeV (left plot) and  $m_{\Sigma_d} = 2200$  GeV (right plot) and  $\mathcal{L} = 3000\text{fb}^{-1}$  in all cases.

tion of them can be stopped inside the detector itself. Their late time decays can be observed in the intervals between the collisions of proton beams [50, 51]. These kind of searches are characterized by rather low efficiencies, in particular because of the low, namely  $\lesssim 10\%$ , fractions of stopped particles; as a consequence one should focus on the regions in which the number of decays outside the pixel/tracker regions is maximal, possibly renouncing to a statistically significant number of events inside the detector. So searches for stopped particles are in some sense complementary to the searches discussed in this work. At the same time, as can be noted e.g. in fig. (4), (5), in the regions where the number of particles decaying outside the detector is maximal, the isolines of DM lifetime and relic density cross at values of the branching ratios of order 0.5 and thus a contemporary detection of both decays of  $\Sigma_d$  is feasible provided the presence of statistically relevant population of stopped particles.

This possibility is confirmed by the outcome of the analysis reported in tab. (2), where a benchmark with  $(m_\psi, m_{\Sigma_d}) = (500, 1000)$  GeV has been considered and the couplings set

Part of detector	Total	$\Sigma \rightarrow DM$	$\Sigma \rightarrow \text{SM only}$
$\mathcal{L} = 25\text{fb}^{-1}$			
Pixel	31	0	31
Tracker	63	0	63
Out	454	1	453
$\mathcal{L} = 300\text{fb}^{-1}$			
Pixel	378	0	378
Tracker	752	1	751
Out	5445	6	5439
$\mathcal{L} = 3000\text{fb}^{-1}$			
Pixel	3785	4	3781
Tracker	7522	8	7514
Out	54446	57	54389

**Table 1:** Number of decay events, total as well as separately in the two kind of decay channels (DM or SM only), which is expected to be observed, in the three detection regions, at the indicated values of the luminosity, for a  $\Sigma_d$  production scenario corresponding to the benchmark set of masses  $m_{\Sigma_d} = 800$  GeV and  $m_\psi = 10$  GeV. The coupling  $\lambda$  and  $\lambda'$  have been chosen in such a way that the DM achieves the correct relic density, through the freeze-in mechanism, and its lifetime is  $10^{28}$  s, just beyond present ID limits. The values of  $\lambda$  and  $\lambda'$  are, respectively,  $1.8 \times 10^{-11}$  and  $5.5 \times 10^{-10}$ .

Part of detector	Total	$\Sigma \rightarrow DM$	$\Sigma \rightarrow \text{SM only}$
$\mathcal{L} = 25\text{fb}^{-1}$			
Pixel	0	0	0
Tracker	0	0	0
Out	178	19	159
$\mathcal{L} = 300\text{fb}^{-1}$			
Pixel	0	0	0
Tracker	0	0	0
Out	2133	222	1911
$\mathcal{L} = 3000\text{fb}^{-1}$			
Pixel	0	0	0
Tracker	0	0	0
Out	21334	2225	19109

**Table 2:** The same as tab. (1) but for  $m_\Sigma = 1$  TeV,  $x = 0.5$  and the couplings  $\lambda$  and  $\lambda'$  set to, respectively,  $1.2 \times 10^{-12}$  and  $3.6 \times 10^{-12}$ , in order to achieve the correct DM relic density and a DM lifetime of  $10^{28}$  s.

in order to achieve, besides the correct DM relic density, a lifetime of the DM of  $10^{28}$  s and a branching ratio of decay of  $\Sigma$  into DM of approximately 10%. For luminosities above  $300 \text{ fb}^{-1}$ , a sizable number of events could be observed in both the decay channels of  $\Sigma_d$ , possibly compensating the low efficiency in the detection of stopped particles. In order to

Part of detector	Total	$\Sigma \rightarrow DM$	$\Sigma \rightarrow \text{SM only}$
$\mathcal{L} = 25\text{fb}^{-1}$			
Pixel	49	8	41
Tracker	58	9	49
Out	2	0	2
$\mathcal{L} = 300\text{fb}^{-1}$			
Pixel	585	92	493
Tracker	692	109	583
Out	25	4	21
$\mathcal{L} = 3000\text{fb}^{-1}$			
Pixel	5848	925	4923
Tracker	6923	1094	5829
Out	250	40	210

**Table 3:** The same as tab. (1) but for  $m_\Sigma = 1\text{TeV}$ ,  $x = 10^{-6}$  and the couplings  $\lambda$  and  $\lambda'$  set to, respectively,  $6.5 \times 10^{-10}$  and  $1.5 \times 10^{-9}$ . For this choice of parameters  $Br(\Sigma_d \rightarrow DM) \sim 0.15$  and the DM relic density is entirely achieved through the freeze-in mechanism. The DM lifetime instead exceeds of many orders of magnitude the sensitivity of present and next future detectors.

quantitatively explore this scenario an analysis accounting for the typology of decay products of  $\Sigma_d$  as well as a simulation of the detector are however needed. This is beyond the scope of this work and will be left to a future study.

The contemporary detection of both decay channels of  $\Sigma_d$  can be feasible as well at very low values of  $x$ , thus corresponding to very light DM particles. Indeed in such a case it is possible to set the two couplings  $\lambda$  and  $\lambda'$  to comparable values without conflicting with ID constraints because of the strong enhancement, namely  $\propto x^{-5}$  of the DM lifetime. We also notice that higher values of the coupling  $\lambda$  are favored by the DM relic density since it tends to be suppressed as  $x$ . In such scenario we thus expect  $\Sigma_f$  particles to be relatively short-lived and thus most of the decay events happen in the pixel/tracker region. This is confirmed by the results shown in tab. (3) in which we have considered a benchmark model with the very low value  $x = 10^{-6}$ . As we expected, most of the decay events lie in the inner detector with statistically relevant populations in both the decay channels. For luminosities above  $300\text{fb}^{-1}$  it is nonetheless possible to observe more than 10 escaping tracks; the LHC thus provides an optimal reconstruction of the properties of the scalar field. On the other hand for the very low value of  $x$  considered the Indirect Detection of DM is not possible since its lifetime largely exceeds present and next future experimental sensitivity. As a consequence, in this kind of setup, LHC is the only probe of the model under consideration.

### 3.2 EW-charged scalar

In this section we present a similar analysis for  $\Sigma_{e,\ell}$ -type scalar field. We will first assume, analogously to the previous scenario, that the two components of the  $SU(2)_L$  doublet are exactly degenerate in mass, such that the analysis can be carried out with the exact same steps as before.

The case in which, instead, a sizable mass splitting is present is also phenomenologically



intriguing. Indeed one of the components of  $\Sigma_\ell$  is electrically neutral and remains undetectable at LHC in case of decays outside the Pixel/Tracker region, thus behaving like an additional DM component. Additional interesting collider signatures can arise in the case in which both the components are accessible to LHC production and decays in W boson (either on- or off-shell) are allowed. We will comment on this possibility at the end of this subsection.

We show in fig. (6) the production cross-section of the  $\Sigma_\ell$  and  $\Sigma_e$  type fields, compared with the one of  $\Sigma_d$ . As we can see the production cross-sections are sensitively lower, with respect to the colored case, with a maximal mass reach, corresponding to the high luminosity upgrade of LHC, of approximately 1400 GeV. At the same time the limits from detector stable

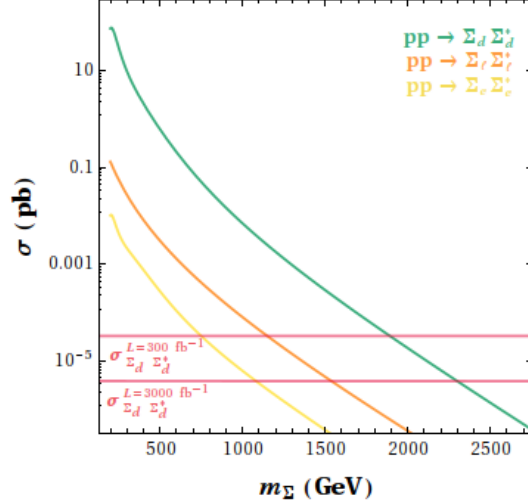


**Figure 6:** NLO cross-section for several kinds of  $\Sigma_f$  field, namely  $\Sigma_d$ ,  $\Sigma_\ell$  and  $\Sigma_e$ . We report as well the minimal value of the production cross-section, for two values of the luminosity, namely 300 and 3000  $\text{fb}^{-1}$ , needed to give 5 pairs of particles.

particles are substantially relaxed with respect to the case of colored particles so that we can consider values of the mass as low as 300 – 400 GeV.

We also notice that the production cross-section of  $\Sigma_\ell$  pairs is sensitively larger with respect to the case of a  $SU(2)_L$  singlet. This enhancement is substantially due to the process  $pp \rightarrow \Sigma_\ell^\pm \Sigma_\ell^0$ , with  $\Sigma_\ell^\pm$  and  $\Sigma_\ell^0$  being, respectively, the electrically charged and neutral components of the  $SU(2)$  doublet. On the other hand the increase in the expected number of events depends on the lifetime of  $\Sigma_\ell$ . It is indeed maximal at shorter lifetimes, when the scalar field decays prevalently in the inner detector, since displaced vertices can be detected both for electrically charged and neutral mother states, while it is more moderate at the longest lifetimes since only the charged component of the  $SU(2)_L$  doublet can manifest as metastable tracks while the neutral one escapes detection.

Fig. (7) and (8) show the LHC reach, in the three detection regions, as function of the couplings  $\lambda$  and  $\lambda'$  and for some fixed values of  $x$ , for two values of  $m_{\Sigma_{\ell,e}}$ , namely 400 and 800 GeV. In the lower mass scenario it is again present an upper bound on the lifetime of the scalar field coming from current searches of disappearing tracks. Notice that this last limit is stronger in the case of  $\Sigma_\ell$  type field as consequence of the higher cross-section at a given value of the mass (see [42] for details.).

Contrary to the colored case it is possible to have sizable or even dominant contribution



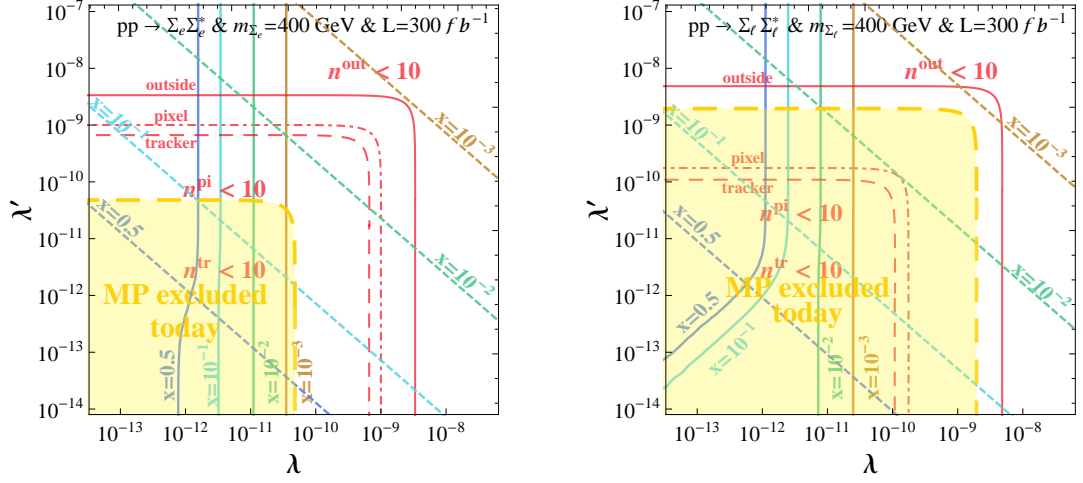


**Figure 7:** LHC reach, in the plane  $(\lambda, \lambda')$ , in the Pixel (red dot-dashed lines), Tracker (red dashed lines) and outside the detector (red solid lines), for an integrated luminosity of  $300\text{fb}^{-1}$  for a  $\Sigma_e$  (left panel) and a  $\Sigma_\ell$  (right panel) scalar field of mass 400 GeV. The solid lines represent the cosmological value of the DM relic density for  $x = \{10^{-3}, 10^{-2}, 0.1, 0.5\}$ , while the short-dashed lines represent a reference value of  $10^{28}\text{s}$ , approximately corresponding to the current experimental sensitivity on the DM lifetime for the considered set of values of  $x$ . The yellow region below the thick long-dashed yellow line is excluded by searches of metastable particles.

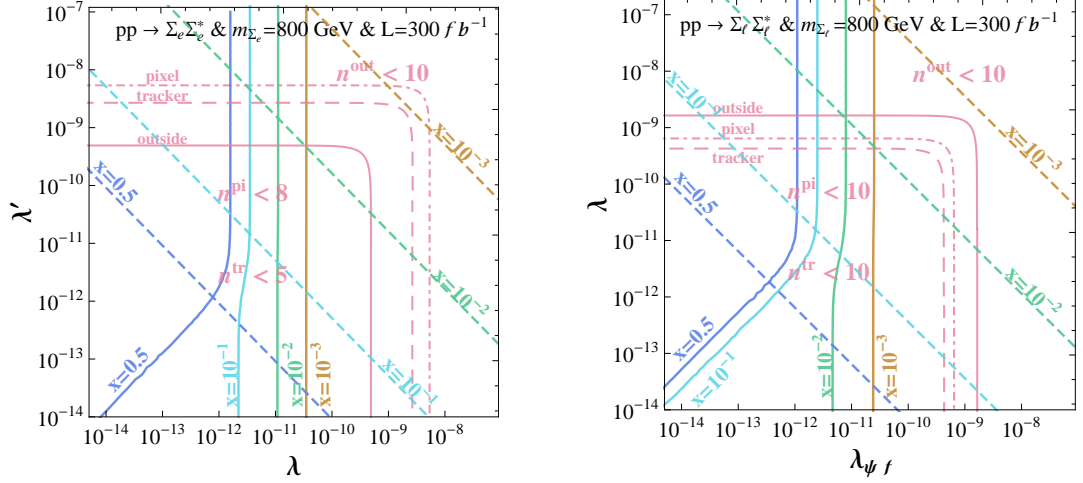


**Figure 8:** The same as fig. (7) but for  $m_{\Sigma_{e,\ell}} = 800\text{ GeV}$ .

from the SuperWIMP mechanism at masses accessible to the LHC production. However, as evident from the plot, this occurs only at very small values of the couplings, such that the decays of the scalar field occur substantially only outside the detector.

We have as well reformulated our results in the plane  $(\text{BR}(\Sigma_f \rightarrow \text{DM}) - \Gamma_\Sigma^{-1})$ . As evident

from fig. (9) and (10) the LHC “double” detection region defined in the previous sections is extremely narrow, as consequence of the lower number of expected events, due to the lower production cross-sections, and it is already closed, for masses of 800 GeV, in the case of  $\Sigma_e$ -type field, which thus features extremely poor detection prospects. We also notice that the crossing of curves of the relic density and the DM lifetime occurs, in the double detection strip, at values of the branching ratio at most of the order of  $10^{-3}$  which again makes very difficult (likely impossible) the detection of the decay channel of  $\Sigma_{\ell,e}$  into DM.

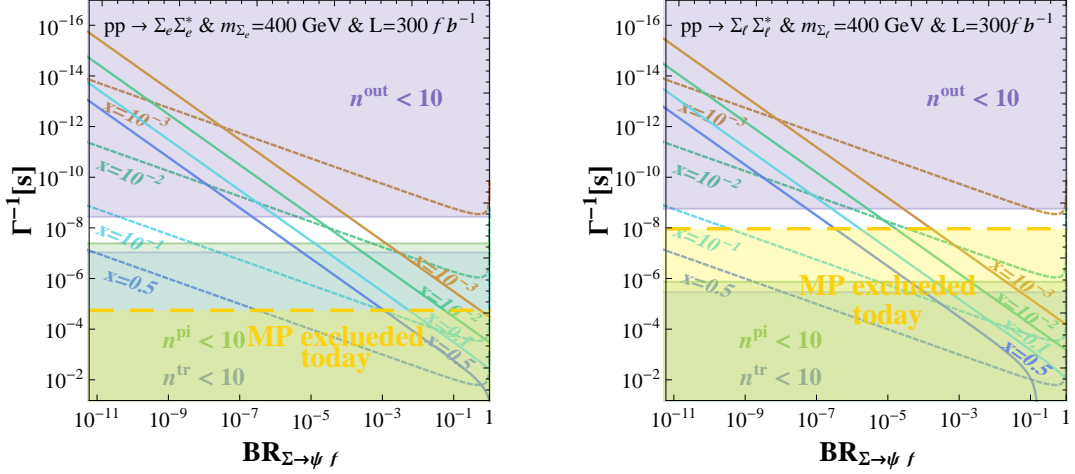


**Figure 9:** LHC reach for  $\Sigma_e$  (left) and  $\Sigma_\ell$  (right) in the plane  $(Br(\Sigma_{e,\ell} \rightarrow \text{DM}), \Gamma_\Sigma^{-1})$  for integrated luminosity of  $300\text{fb}^{-1}$  and  $m_{\Sigma_{e,\ell}} = 400$  GeV. The violet, green and blue region represent the regions where less than 10 events are expected, respectively in the ‘outside’, tracker and pixel regions. The ‘double detection’ region, defined in the main text, is thus the white strip between the shaded regions. The solid and dashed lines give again the cosmological relic density and the reference DM lifetime for the set  $x = \{10^{-3}, 10^{-2}, 0.1, 0.5\}$ . The yellow region below the thick dashed yellow line is excluded by current searches of metastable particles.

Analogously to the previous section, we have investigated the prospects of detection of  $\Sigma_{\ell,e}$  from a more quantitative perspective focussing on a benchmark set of parameters. We have indeed considered the pair production of a  $\Sigma_\ell$  particle with an assignment of (10,400) GeV for  $(m_\psi, m_{\Sigma_\ell})$  and fixed the couplings to give the correct relic density and a lifetime compatible with experimental limits. As evident from the results reported in table (4) the number of expected events is drastically reduced with respect to the colored case. A statistically relevant number of decay events both in the inner and outer part of the detector appears only at luminosities above  $300\text{fb}^{-1}$ . An eventual discovery of this scenario will thus require more time with respect to the case of color charged scalar field. We notice moreover that the low production cross section, combined with the low branching ratio  $\sim 10^{-3}$ , does not allow for any event with  $\Sigma_\ell$  decaying into DM, even considering a high luminosity upgrade of the LHC. Since our choice of the mass of  $\Sigma_\ell$  corresponds to the maximal cross-section available, it appears evident that, in the case of  $\Sigma_f$  charged only with respect to electroweak interactions, it will not be possible to identify at LHC the peculiar feature of our model, namely the presence of two (i.e. DM+SM and SM only) decay channels.

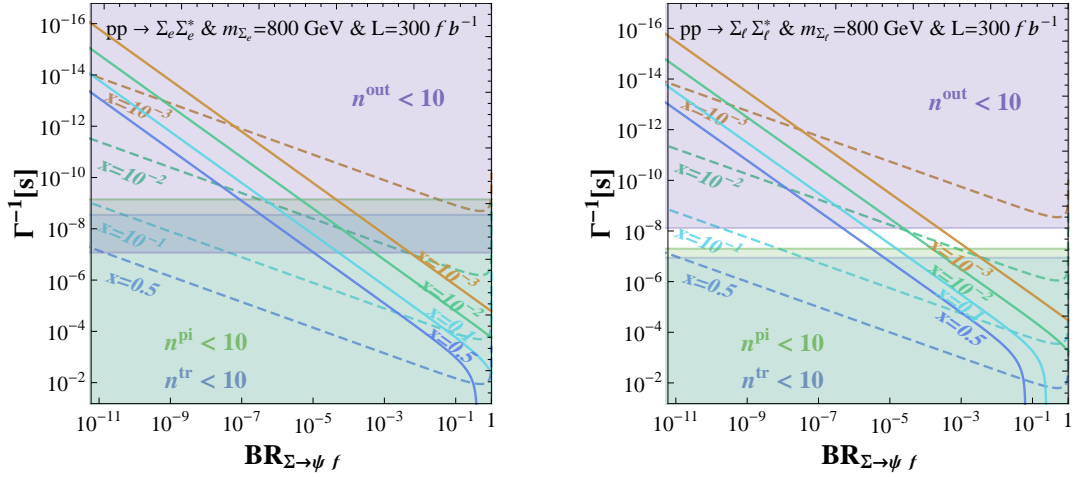


**Figure 10:** The same as fig. (9) but for  $m_{\Sigma_{e,\ell}} = 800$  GeV. A 'double detection' region is present only in the case of  $\Sigma_\ell$ -type field.

Part of detector	Total	$\Sigma \rightarrow DM$	$\Sigma \rightarrow SM$ only
$\mathcal{L} = 25\text{fb}^{-1}$			
Pixel	1	0	1
Tracker	2	0	2
Out	23	0	23
$\mathcal{L} = 300\text{fb}^{-1}$			
Pixel	14	0	14
Tracker	26	0	26
Out	270	0	270
$\mathcal{L} = 3000\text{fb}^{-1}$			
Pixel	135	0	135
Tracker	260	0	260
Out	2705	0	2705

**Table 4:** Number of decay events, total as well as separately in the two kind of decay channels (DM or SM only), expected in the three detection regions at the LHC for the indicated values of luminosity. The benchmark chosen consist in a  $\Sigma_\ell$ -type field with mass of 400 GeV while the DM mass is set to 10 GeV. The pair  $(\lambda, \lambda')$  has been fixed to  $(5 \times 10^{-12}, 10^{-9})$ .

Analogously to the colored scenario we can consider signals outside the double detection regions. In the high lifetime region only the decay channel into SM particles might be accessible to possible searches of stopped particles since the small number of events, consequence of the low production cross section, does not allow to have a statistically relevant number of events in both the decay channels<sup>5</sup>. Alternatively we can consider very low values of the DM

<sup>5</sup>We also notice that there are not, at the moment, searches of only electroweakly interacting stopped particles. On general grounds we expect a lower detection efficiency with respect to the case of color interaction.

Part of detector	Total	$\Sigma \rightarrow DM$	$\Sigma \rightarrow SM$ only
$\mathcal{L} = 25\text{fb}^{-1}$			
Pixel	1	1	0
Tracker	2	1	1
Out	8	4	4
$\mathcal{L} = 300\text{fb}^{-1}$			
Pixel	12	6	6
Tracker	27	14	13
Out	94	48	46
$\mathcal{L} = 3000\text{fb}^{-1}$			
Pixel	120	62	58
Tracker	270	139	131
Out	941	484	457

**Table 5:** Number of decay events, total as well as separately in the two kind of decay channels (DM or SM only), which is expected in the three detection regions at the LHC for the indicated values of luminosity. The benchmark chosen consist in a  $\Sigma_\ell$ -type field with mass of 800 GeV while the DM mass is set to  $8 \times 10^{-4}$  GeV. The pair  $(\lambda, \lambda')$  has been fixed to  $(8 \times 10^{-10}, 7.8 \times 10^{-10})$  and corresponds to a lifetime many orders of magnitude above current and next future experimental sensitivity. No ID detection is thus expected in this case.

mass in order to evade ID constraints and for  $x \sim 10^{-6}$  it might be again possible to observe both the  $\Sigma_\ell$  decay channels, renouncing however to the possibility of next future detection of DM decays in cosmic rays. A possible outcome in this kind of scenario is reported in tab. (5), where it is shown the number of expected observed decay events in the case of  $\Sigma_\ell$ -type field with mass of 800 GeV and for a very low value of the DM mass corresponding to  $x = 10^{-6}$ . The value of the  $(\lambda, \lambda')$  pair, respectively  $8 \times 10^{-10}$ ,  $7.8 \times 10^{-10}$ , guarantees the correct DM relic density, through the freeze-in mechanism, and a branching fraction of decay of the scalar field into DM of approximately 50%. Although the choice of the parameters is substantially analogous to the low mass benchmark studied in the case of color charged scalar (the lifetimes of the scalar field differ approximately by a factor 2) the majority of the events now lie in the “outside” region. This is due to the fact the  $\Sigma_{\ell,e}$  are more boosted with respect to colored scalars. At the higher luminosities we have anyway a number of events in the inner detector, for both decay channels, satisfying our discovery requirement. We have thus again a good capability for LHC of providing information on the model under consideration, renouncing however at any prospects of indirect detection of the decays of the DM.

We conclude this section describing how the LHC signals may result altered, in the  $\Sigma_\ell$  scenario, in the presence of a sizable mass splitting in the EW multiplet. As already mentioned in this case the heaviest component of the doublet dominantly decays into the lighter one and a W boson (or into two quarks/leptons) and these decays result prompt for mass-splitting above  $\sim 1$  GeV. Contrary to the colored case, we can have a sizable production of the heavy component through the process  $pp \rightarrow \Sigma_\ell^\pm \Sigma_\ell^0$ , being mediated by the W boson, which can account for  $\sim 50\%$  of the total production cross-section even for sizable mass splittings. The range of signals results therefore enriched if the detection of the products of the prompt decays

of the heavy component of the doublet is possible.

In the case  $m_{\Sigma^\pm} > m_{\Sigma^0}$  the decays  $\Sigma^\pm \rightarrow \Sigma^0 f \bar{f}'$  produce displaced vertices accompanied by prompt leptons and jets, for short lifetimes of  $\Sigma^0$ , or a signal consisting of jet/leptons+missing energy, customarily studied in supersymmetric setups [52, 53], in the case that  $\Sigma^0$  decays outside the inner detector<sup>6</sup>. In the opposite case  $m_{\Sigma^\pm} < m_{\Sigma^0}$  prompt jets/leptons are associated to displaced vertices or metastable tracks.

## 4 Discussion

In this section we summarize the outcome of the previous analysis and discuss in greater detail whether an hypothetical next future LHC signal can unambiguously discriminate the underlying particle physics scenario.

We show in fig. (11) and (12) the LHC reach, in the two scenarios of  $\Sigma_d$ - and  $\Sigma_\ell$ -type field, as function of the mass of the scalar field and of the coupling  $\lambda'$ , for the two assignments of the DM mass of 10 and 100 GeV. The luminosity has been set to  $300\text{fb}^{-1}$ . The coupling  $\lambda$  has been determined as function of the other parameters, using eq. (2.5), (2.6) and (2.7), according the requirement of the correct DM relic density.

The red, blue and green lines in the plots correspond to the observation of 10 events respectively in the Tracker, Pixel and outside the detector region. The green region comprised between this lines is the “double detection” region, in which the observation of at least 10 events in the inner detector and at least 10 escaping tracks. Above this region only displaced vertices can be observed at a statistically relevant amount while below metastable tracks are the only visible signal. The yellow regions in the plots are already excluded, for the considered values of the DM mass, by constraints from DM indirect detection<sup>7</sup>. As evident the possibility of “double” LHC detection is already ruled out for DM masses above 100 GeV in the case of colored scalar and for masses above 10 GeV in the case of EW charged scalar. Nevertheless for the colored case, as can be seen in the left panel of fig. (11) as well as in the benchmark in Table 1, the future indirect detection region just below the present bound lies exactly in the double detection corner for a DM mass of 10 GeV and  $m_\Sigma < 1500$  GeV and in that case possibly all the four parameters of the model could be within reach in the next future. The possibility of observing only displaced vertices is disfavored as well by ID for these values of the DM mass, ad exception of the highest value of the scalar field mass, at the boundaries of the LHC reach. The more severe exclusion in this last case is due to the fact that the production of lighter scalar particles is considered, in turn implying higher decay rates for the DM.

We can now investigate in more detail which kind of information can be inferred from an hypothetical future LHC signal. At high DM masses, namely above 100 (10) GeV in the colored (only electroweakly interacting)  $\Sigma_f$  scenario, the only signal which can be expected are metastable tracks. In such case it will be possible to give a lower bound on the scalar field lifetime or perhaps to measure it, although maybe with less precision with respect to a double detection scenario, from the decay of stopped  $\Sigma_f$ . From this it may be possible to determine the sum  $\lambda^2 + \lambda'^2$  while, in absence of observation of the decay processes, it is

---

<sup>6</sup>Notice that we could as well consider monojet + missing energy signals in the case of long lived pair produced  $\Sigma_\ell^0$ , totally analogous to the DM pair production scenarios. However in our setup pair production of  $\Sigma_\ell^0$  occurs only through a strongly off-shell Z-boson giving a rather weak signal [2, 54].

<sup>7</sup>Notice that our bounds from ID detection are rather conservative. In the case of  $\Sigma_{\ell,e}$ -type field we can obtain, for example, weaker bounds assuming decays only in some flavour states like, e.g.,  $\tau$  leptons.

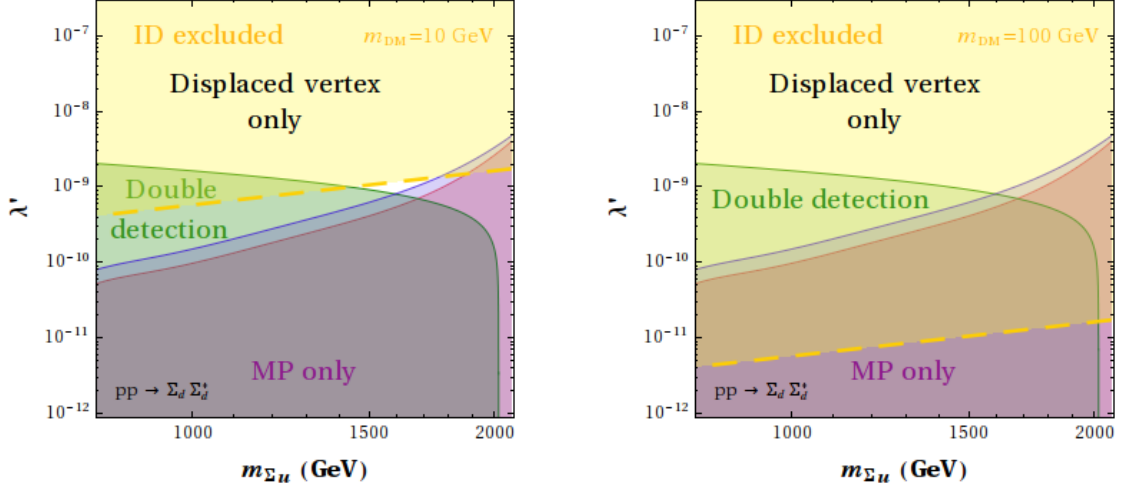


**Figure 11:** Summary of the possible observed signals at LHC, at  $\mathcal{L} = 300\text{fb}^{-1}$ , for a  $\Sigma_d$ -type field, as function of its mass and the coupling  $\lambda'$ . The other coupling,  $\lambda$ , has been fixed in order to reproduce the correct DM relic density while the DM mass has been set to 10 GeV (left plot) and 100 GeV (right plot). The red, blue and green lines correspond to the observation of 10 events respectively in the Tracker, Pixel and outside the detector region. In the “double” detection region, the green shaded region between this lines, a number  $\geq 10$  of decay events in the Pixel and the Tracker and more than 10 tracks leave the detector. The yellow shaded region, above the thick yellow dashed line, is excluded by constraints from indirect detection of DM decay.

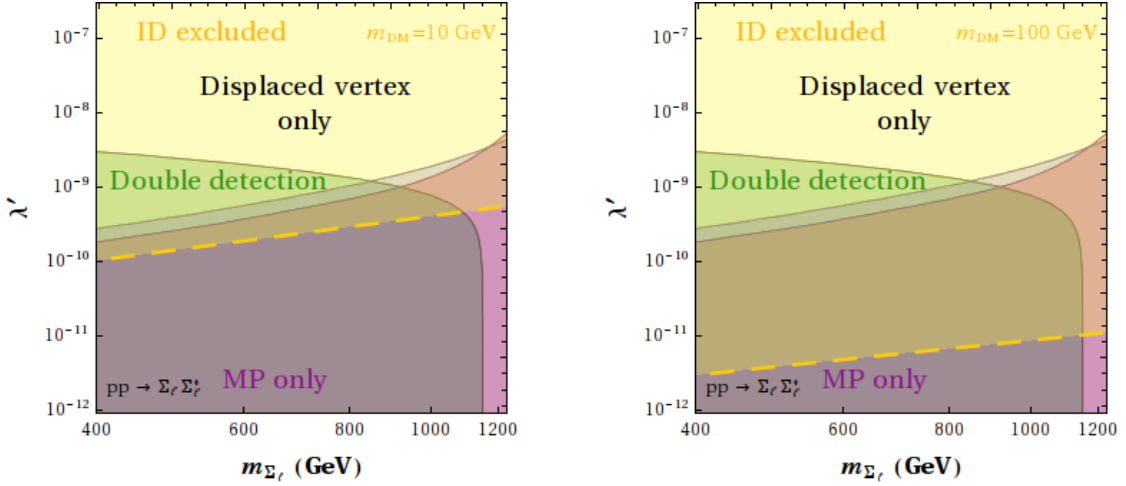


**Figure 12:** The same as fig.(11) but for the case of a  $\Sigma_\ell$ -type field.

not possible to determine the single values of the two couplings, which could allow to infer the DM production mechanism. This task could be achieved in case of an Indirect Detection

of dark matter decay which would provide, besides the value of the DM mass, information on a different combination of the two couplings, namely their product  $\lambda\lambda'$ . The complete identification of the model could then be achieved by verifying that the DM relic density, computed with the reconstructed parameters, matches the cosmological value.

At intermediate DM mass scales the LHC “double” detection region is instead still viable. This scenario guarantees the optimal reconstruction of the lifetime of the scalar field, as well as its mass which can be inferred by the cross section and by the energy of the decay products. As already pointed out these informations alone do not allow to infer the DM relevant properties like the mass, which it is in any case not accessible at the LHC, and the production mechanism. Indeed the latter would require the knowledge of the single values of the couplings  $\lambda$  and  $\lambda'$  while the lifetime of  $\Sigma_f$  depends on the sum  $\lambda^2 + \lambda'^2$ . The two couplings could be singularly inferred in case it is possible to distinguish, through the decay products in the displaced vertices, the two decay channels of the scalar field. However our study based on the relative branching fractions of the two decay channels of the scalar fields, confirmed from a quantitative perspective by the study of the two benchmarks reported in tab. (1) and (4), has shown that only the pure SM decay channel is accessible to LHC detection. In this case it is possible to infer, from the determination of the lifetime of the scalar field, only the value of  $\lambda'$  (assuming a negligible branching fraction of decay into DM). A LHC signal only can thus neither provide evidence of the existence of the DM nor information on its production mechanism. A correlation with a DM ID signal is again mandatory for determining the remaining parameters. In both the scenarios proposed above the capability of full determination of the model under consideration is hence limited to the regions of the parameters space which lie in proximity of the current experimental sensitivity to DM Indirect Detection.

For very low DM masses, LHC is instead the only probe of the model under consideration while ID is not achievable (as a consequence, bounds like the ones shown in fig. (11) and (12), are completely evaded). On the contrary the two branching fractions of decay into the scalar field, namely the one into DM+SM and only SM, can be comparable within the double detection region. This statement is again confirmed at the quantitative level by the study of two benchmarks, one for colored and one for only EW interacting scalar, reported in tab. (3) and (5), which show the presence of statistically relevant number of events, for both the two decay channels, in the inner detector as well as in the “outside” region. In case of identification of the two decay channels it is possible to infer the values of  $\lambda$  and  $\lambda'$  as well as the  $m_{\Sigma_f}$ . The DM mass is instead not directly accessible from observations but might be determined from the requirement of the correct relic density, given its proportionality to  $x = m_\psi/m_{\Sigma_f}$ .

We remark anyway that the capability of disentangling the decay channels of the scalar field is actually model dependent since, according to which of the operators in (2.1) and (2.2) determine the decay processes of  $\Sigma_f$ , we might have scenarios with very different decay products in the two channels (for example in the case of  $\Sigma_\ell$  field we can have a decay into DM and a charged lepton opposed to a decay into two jets triggered by the coupling  $\lambda_{2,3\ell}$ ) as well as rather similar signals, e.g. in the case in which the scalar field decays into a neutrino and another SM fermion. We also remark that the various kinds of final states, e.g. jets, leptons etc..., possibly emerging from displaced vertices have not the same capability of reconstruction, at a given lifetime (see e.g. [13] for a discussion). In order to properly address this issue a refinement of our analysis, including a simulation of the detector, is required.

The statements discussed until now substantially hold for all the assignments of the SM charge of the  $\Sigma_f$  particle. In absence of a detector analysis, sensitive to the decay products,



the main difference is between the cases of colored or only electroweakly charged  $\Sigma_f$  with the latter requiring higher luminosities for a discovery and featuring a more limited mass reach, in view of the lower production cross-section. In the case of colored mediator one could consider complementary searches, with respect to the one discussed in this paper, relying on the possibility of observing very late decays of  $\Sigma_f$  particles stopped in the detector. At these very long lifetimes the observation of both decay channels of  $\Sigma_f$  is compatible with constraints from DM phenomenology. Our study reported in tab. (2) shows that this possibility is potentially feasible even once the actual low efficiencies in this kind of searches are accounted for. On the other hand we remark again that in order to properly determine whether the different decay channels can be discriminated a simulation of the detector is mandatory and that a definite statement is left to a future study. In case of possible identifications of the two decay channels it is again possible to determine their relative branching fractions and then directly the couplings  $\lambda$  and  $\lambda'$ .

## 5 Conclusions

We have considered the LHC detection prospects of a very simple and economical extension of the Standard Model featuring a decaying Majorana fermion as DM candidate and a metastable scalar field with non-trivial quantum numbers under the SM gauge group. The potential LHC signal is constituted by the observation of the displaced decays of the scalar field, either into the DM and a SM fermion or into two SM fermions, or of the scalar field itself as disappearing track escaping the detector. We have investigated the possibility of detecting this kind of signals in the regions of the parameters space favored by the requirement of the correct DM relic density and a future Indirect Detection of the DM decays.

In the case of color charged scalar field a statistically relevant population of both displaced vertices and metastable tracks might be observed in next future 14 TeV LHC run up to masses of the order of 1500 GeV and up to approximately 2200 considering a high luminosity run; however bounds from DM Indirect Detection already exclude the possibility of "double" detection for DM masses above 100 GeV, leaving open only a possible detection of metastable tracks. In the parameter region corresponding to the "double" LHC detection unfortunately only the decay channel into just SM fermions is accessible to observation, since the branching ratio of the scalar field into DM is of the order  $\leq 10^{-2} - 10^{-3}$ . The two decay channels of the  $\Sigma_f$  field might be instead contemporarily observed in the case of very long  $\Sigma_f$  lifetimes, with negligible amount of events in the inner detector, considering the possibility that a fraction of  $\Sigma_f$  can be stopped in the detector material and decay at later time. This possibility should be investigated through a dedicated study. The contemporary detection of the two decay channels of  $\Sigma_f$  can occur as well at very low, i.e.  $\ll 1$  GeV DM masses. In this case there would be the observation of mostly displaced vertices in the inner detector, while DM decays in Indirect Detection are unfortunately beyond present and future observational capabilities because of the extremely long DM lifetimes.

In the case in which, instead,  $\Sigma_f$  features only electroweak interactions the maximal mass reach is limited to approximately 1400 TeV and the high luminosity upgrade is most likely needed to probe the parameters space of model. Because of the lower masses of  $\Sigma_f$  involved in the analysis the bounds from DM ID are more severe, with respect to the case of a colored scalar field, such that under the most conservative assumptions the "double" LHC detection is not possible for DM masses above 10 GeV. There are as well poorer prospects of detection of stopped particles because of the lower number of events and of stopping probability. The



scenario of contemporary detection of the two decay channels at very low DM masses is instead feasible although kinematic effects imply, contrary to the colored case, a greater number of decays in the outer detector region. The range of possible signals is enriched in the case the scalar field is a  $SU(2)_L$  doublet with a mass splitting between the components. In particular, in the case of  $\Sigma_\ell$  type field, with lighter neutral component, the signals presented above can be accompanied as well by conventional missing energy signatures and prompt tracks.

In most of the parameter space of the scenario presented, LHC experiments and Indirect Detection observations provide complementary information on the model and both signals are necessary in order to confirm the identity of the Dark Matter and verify the production mechanism. In particular if the mass of the Dark Matter is in the 1-10 GeV range and the  $\Sigma_f$  scalar within the kinematical reach of the next LHC run, i.e. below 1600 GeV for the colored case or 1100 GeV for the EW case, there is a clear chance to obtain multiple signals in the very near future.

## Acknowledgments

The authors thank Marco Nardecchia for enlightening discussions.

The authors acknowledge partial support from the European Union FP7 ITN-INVISIBLES (Marie Curie Actions, PITN-GA-2011-289442).

## References

- [1] **ATLAS Collaboration** Collaboration, *Search for New Phenomena in Monojet plus Missing Transverse Momentum Final States using 10fb-1 of pp Collisions at  $\sqrt{s}=8$  TeV with the ATLAS detector at the LHC*, Tech. Rep. ATLAS-CONF-2012-147, CERN, Geneva, Nov, 2012.
- [2] **CMS Collaboration** Collaboration, *Search for new physics in monojet events in pp collisions at  $\sqrt{s}=8$  TeV*, Tech. Rep. CMS-PAS-EXO-12-048, CERN, Geneva, 2013.
- [3] G. Arcadi and L. Covi, *Minimal Decaying Dark Matter and the LHC*, *JCAP* **1308** (2013) 005, [[arXiv:1305.6587](#)].
- [4] T. Han, Z. Si, K. M. Zurek, and M. J. Strassler, *Phenomenology of hidden valleys at hadron colliders*, *JHEP* **0807** (2008) 008, [[arXiv:0712.2041](#)].
- [5] K. Ishiwata, T. Ito, and T. Moroi, *Long-Lived Unstable Superparticles at the LHC*, *Phys.Lett. B* **669** (2008) 28–33, [[arXiv:0807.0975](#)].
- [6] S. Chang and M. A. Luty, *Displaced Dark Matter at Colliders*, [[arXiv:0906.5013](#)].
- [7] P. Meade, S. Nussinov, M. Papucci, and T. Volansky, *Searches for Long Lived Neutral Particles*, *JHEP* **1006** (2010) 029, [[arXiv:0910.4160](#)].
- [8] P. Meade, M. Reece, and D. Shih, *Long-Lived Neutralino NLSPs*, *JHEP* **1010** (2010) 067, [[arXiv:1006.4575](#)].
- [9] S. Bobrovskiy, W. Buchmuller, J. Hajer, and J. Schmidt, *Quasi-stable neutralinos at the LHC*, *JHEP* **1109** (2011) 119, [[arXiv:1107.0926](#)].
- [10] J. Heisig and J. Kersten, *Production of long-lived staus in the Drell-Yan process*, *Phys.Rev. D* **84** (2011) 115009, [[arXiv:1106.0764](#)].
- [11] P. Ghosh, D. E. Lopez-Fogliani, V. A. Mitsou, C. Munoz, and R. Ruiz de Austri, *Probing the  $\hat{t}\bar{t}j$ -from- $\hat{t}\bar{t}j$  supersymmetric standard model with displaced multileptons from the decay of a Higgs boson at the LHC*, *Phys.Rev. D* **88** (2013) 015009, [[arXiv:1211.3177](#)].

- [12] J. Heisig and J. Kersten, *Long-lived staus from strong production in a simplified model approach*, *Phys.Rev.* **D86** (2012) 055020, [[arXiv:1203.1581](#)].
- [13] P. W. Graham, D. E. Kaplan, S. Rajendran, and P. Saraswat, *Displaced Supersymmetry*, *JHEP* **1207** (2012) 149, [[arXiv:1204.6038](#)].
- [14] J. Heisig, J. Kersten, B. Panes, and T. Robens, *A survey for low stau yields in the MSSM*, *JHEP* **1404** (2014) 053, [[arXiv:1310.2825](#)].
- [15] M. Cirelli, F. Sala, and M. Taoso, *Wino-like Minimal Dark Matter and future colliders*, [arXiv:1407.7058](#).
- [16] J. L. Feng and B. T. Smith, *Slepton trapping at the large hadron and international linear colliders*, *Phys.Rev.* **D71** (2005) 015004, [[hep-ph/0409278](#)].
- [17] M. Hirsch, W. Porod, and D. Restrepo, *Collider signals of gravitino dark matter in bilinearly broken  $R$ -parity*, *JHEP* **0503** (2005) 062, [[hep-ph/0503059](#)].
- [18] N. Arkani-Hamed and N. Weiner, *LHC Signals for a SuperUnified Theory of Dark Matter*, *JHEP* **0812** (2008) 104, [[arXiv:0810.0714](#)].
- [19] L. J. Hall, K. Jedamzik, J. March-Russell, and S. M. West, *Freeze-In Production of FIMP Dark Matter*, *JHEP* **1003** (2010) 080, [[arXiv:0911.1120](#)].
- [20] C. Cheung, G. Elor, L. J. Hall, and P. Kumar, *Origins of Hidden Sector Dark Matter II: Collider Physics*, *JHEP* **1103** (2011) 085, [[arXiv:1010.0024](#)].
- [21] L. Covi, M. Olechowski, S. Pokorski, K. Turzynski, and J. D. Wells, *Supersymmetric mass spectra for gravitino dark matter with a high reheating temperature*, *JHEP* **1101** (2011) 033, [[arXiv:1009.3801](#)].
- [22] M. Endo, K. Hamaguchi, and K. Nakaji, *Probing High Reheating Temperature Scenarios at the LHC with Long-Lived Staus*, *JHEP* **1011** (2010) 004, [[arXiv:1008.2307](#)].
- [23] J. M. Lindert, F. D. Steffen, and M. K. Trenkel, *Direct stau production at hadron colliders in cosmologically motivated scenarios*, *JHEP* **1108** (2011) 151, [[arXiv:1106.4005](#)].
- [24] M. Garny, A. Ibarra, D. Tran, and C. Weniger, *Gamma-Ray Lines from Radiative Dark Matter Decay*, *JCAP* **1101** (2011) 032, [[arXiv:1011.3786](#)].
- [25] M. Garny, A. Ibarra, and S. Vogl, *Dark matter annihilations into two light fermions and one gauge boson: General analysis and antiproton constraints*, *JCAP* **1204** (2012) 033, [[arXiv:1112.5155](#)].
- [26] M. Garny, A. Ibarra, and D. Tran, *Constraints on Hadronically Decaying Dark Matter*, *JCAP* **1208** (2012) 025, [[arXiv:1205.6783](#)].
- [27] R. Barbier, C. Berat, M. Besancon, M. Chemtob, A. Deandrea, et al.,  *$R$ -parity violating supersymmetry*, *Phys.Rept.* **420** (2005) 1–202, [[hep-ph/0406039](#)].
- [28] A. Y. Smirnov and F. Vissani, *Upper bound on all products of  $R$ -parity violating couplings  $\lambda$ -prime and  $\lambda$ -prime-prime from proton decay*, *Phys.Lett.* **B380** (1996) 317–323, [[hep-ph/9601387](#)].
- [29] N. Fornengo, L. Maccione, and A. Vittino, *Constraints on particle dark matter from cosmic-ray antiprotons*, *JCAP* **1404** (2014) 003, [[arXiv:1312.3579](#)].
- [30] A. Ibarra, A. S. Lamperstorfer, and J. Silk, *Dark matter annihilations and decays after the AMS-02 positron measurements*, *Phys.Rev.* **D89** (2014) 063539, [[arXiv:1309.2570](#)].
- [31] **LAT Collaboration** Collaboration, M. Ackermann et al., *Fermi LAT Search for Dark Matter in Gamma-ray Lines and the Inclusive Photon Spectrum*, *Phys.Rev.* **D86** (2012) 022002, [[arXiv:1205.2739](#)].

- [32] **Fermi-LAT Collaboration** Collaboration, M. Ackermann et al., *Search for Gamma-ray Spectral Lines with the Fermi Large Area Telescope and Dark Matter Implications*, *Phys.Rev.* **D88** (2013) 082002, [[arXiv:1305.5597](#)].
- [33] X. Chu, T. Hambye, and M. H. Tytgat, *The Four Basic Ways of Creating Dark Matter Through a Portal*, *JCAP* **1205** (2012) 034, [[arXiv:1112.0493](#)].
- [34] X. Chu, Y. Mambrini, J. Quevillon, and B. Zaldivar, *Thermal and non-thermal production of dark matter via  $Z'$ -portal(s)*, *JCAP* **1401** (2014) 034, [[arXiv:1306.4677](#)].
- [35] M. Klasen and C. E. Yaguna, *Warm and cold fermionic dark matter via freeze-in*, *JCAP* **1311** (2013) 039, [[arXiv:1309.2777](#)].
- [36] M. Blennow, E. Fernandez-Martinez, and B. Zaldivar, *Freeze-in through portals*, [arXiv:1309.7348](#).
- [37] L. Covi, J. E. Kim, and L. Roszkowski, *Axinos as cold dark matter*, *Phys.Rev.Lett.* **82** (1999) 4180–4183, [[hep-ph/9905212](#)].
- [38] J. L. Feng, A. Rajaraman, and F. Takayama, *Superweakly interacting massive particles*, *Phys.Rev.Lett.* **91** (2003) 011302, [[hep-ph/0302215](#)].
- [39] J. L. Feng, A. Rajaraman, and F. Takayama, *SuperWIMP dark matter signals from the early universe*, *Phys.Rev.* **D68** (2003) 063504, [[hep-ph/0306024](#)].
- [40] M. Gomez, C. Jackson, and G. Shaughnessy, *Dark Matter on Top*, [arXiv:1404.1918](#).
- [41] J. Alwall, M. Herquet, F. Maltoni, O. Mattelaer, and T. Stelzer, *MadGraph 5 : Going Beyond*, *JHEP* **1106** (2011) 128, [[arXiv:1106.0522](#)].
- [42] L. Covi and F. Dradi, *Long-Lived stop at the LHC with or without R-parity*, [arXiv:1403.4923](#).
- [43] **CMS Collaboration** Collaboration, S. Chatrchyan et al., *The CMS experiment at the CERN LHC*, *JINST* **3** (2008) S08004.
- [44] **CMS Collaboration** Collaboration, *Search for long-lived particles decaying to final states that include dileptons*, Tech. Rep. CMS-PAS-EXO-12-037, CERN, Geneva, 2014.
- [45] *Search for long-lived, heavy particles in final states with a muon and a multi-track displaced vertex in proton-proton collisions at  $\sqrt{s} = 8\text{TeV}$  with the ATLAS detector.*, Tech. Rep. ATLAS-CONF-2013-092, CERN, Geneva, Aug, 2013.
- [46] S. Asai, K. Hamaguchi, and S. Shirai, *Measuring lifetimes of long-lived charged massive particles stopped in LHC detectors*, *Phys.Rev.Lett.* **103** (2009) 141803, [[arXiv:0902.3754](#)].
- [47] W. Beenakker, R. Hopker, and M. Spira, *PROSPINO: A Program for the production of supersymmetric particles in next-to-leading order QCD*, [hep-ph/9611232](#).
- [48] **ATLAS Collaboration** Collaboration, G. Aad et al., *Searches for heavy long-lived sleptons and R-Hadrons with the ATLAS detector in pp collisions at  $\sqrt{s} = 7\text{ TeV}$* , *Phys.Lett.* **B720** (2013) 277–308, [[arXiv:1211.1597](#)].
- [49] **CMS Collaboration** Collaboration, S. Chatrchyan et al., *Searches for long-lived charged particles in pp collisions at  $\sqrt{s}=7$  and  $8\text{ TeV}$* , *JHEP* **1307** (2013) 122, [[arXiv:1305.0491](#)].
- [50] **ATLAS Collaboration** Collaboration, G. Aad et al., *Search for long-lived stopped R-hadrons decaying out-of-time with pp collisions using the ATLAS detector*, *Phys.Rev.* **D88** (2013) 112003, [[arXiv:1310.6584](#)].
- [51] **CMS Collaboration** Collaboration, S. Chatrchyan et al., *Search for stopped long-lived particles produced in pp collisions at  $\sqrt{s} = 7\text{ TeV}$* , *JHEP* **1208** (2012) 026, [[arXiv:1207.0106](#)].
- [52] **ATLAS Collaboration** Collaboration, G. Aad et al., *Search for direct production of charginos, neutralinos and sleptons in final states with two leptons and missing transverse*

momentum in  $pp$  collisions at  $\sqrt{s} = 8 \text{ TeV}$  with the ATLAS detector, *JHEP* **1405** (2014) 071, [[arXiv:1403.5294](#)].

- [53] **CMS Collaboration** Collaboration, V. Khachatryan et al., *Searches for electroweak production of charginos, neutralinos, and sleptons decaying to leptons and  $W$ ,  $Z$ , and Higgs bosons in  $pp$  collisions at 8 TeV*, [arXiv:1405.7570](#).
- [54] P. J. Fox, R. Harnik, J. Kopp, and Y. Tsai, *Missing Energy Signatures of Dark Matter at the LHC*, *Phys.Rev.* **D85** (2012) 056011, [[arXiv:1109.4398](#)].